Supporting Information For

Different Arsenate and Phosphate Incorporation Effects on the Nucleation and Growth of Iron(III) (Hydr)oxides on Quartz

Chelsea Neil[1], Byeongdu Lee,[2] and Young-Shin Jun[1,] *

[1]*Department of Energy, Environmental and Chemical Engineering,*

Washington University, St. Louis, MO 63130

[2]*X-ray Science Division, Argonne National Laboratory,*

Argonne, IL 60439

E-mail: ysjun@seas.wustl.edu

http://encl.engineering.wustl.edu/

September 2014

Environmental Science and Technology

*To Whom Correspondence Should be Addressed

Summary

Eighteen pages, including experimental and analytical descriptions and 7 Figures.

S1. Sample and Solution Preparations

Cleaning single crystal quartz substrates. After being cut to 1 cm square pieces, quartz substrates were sonicated in acetone for 10 minutes to remove organic contaminants. Substrates were then soaked overnight in a mixture of concentrated sulfuric acid and a commercial oxidizing agent, Nochromix®. Quartz substrates were elevated on their sides to ensure both sides contacted the cleaning solution. Finally, the substrates were rinsed with and stored in deionized water (resistivity > 18.2 MΩ-cm) until the experiments. Substrates were not stored for longer than 1 week. Just before being utilized in GISAXS/SAXS experiments, substrates were rinsed again using ultrapure deionized water.

Solution preparation. The solutions for the systems outlined in Table 1 were created using reagent grade $Fe(NO_3)_3 \cdot 9H_2O$, $NaNO_3$, $Na_2HAsO_4 \cdot 7H_2O$, and $Na_2HPO_4 \cdot 7H_2O$ and ultrapure water. Immediately prior to conducting grazing incidence small angle X-ray scattering (GISAXS), dynamic light scattering (DLS), and other *ex situ* experiments, the salts were weighed (0.0452 g $NaNO_3$, 0.0202 g $Fe(NO_3)_3 \cdot 9H_2O$, 0.0016 g $Na_2HAsO_4 \cdot 7H_2O$, and 0.0013 g $Na_2HPO_4 \cdot 7H_2O$) and stored in 50 mL centrifuge tubes. Ultrapure water was added to the weighed $NaNO_3$ to a volume of 45 mL for the iron only system, or to 40 mL for the systems containing arsenic or phosphate. The tube was shaken to mix the contents. For the arsenic and phosphate systems, 50 mL ultrapure water was added to the arsenic or phosphate salts to create a 10^{-4} M (for 0.0016 g arsenic salt or 0.0013 g phosphate salt) solution, and the tube was shaken. Then 5 mL of the arsenic or phosphate salt solution was added to the 40 mL $NaNO_3$ solution, diluting the arsenate or phosphate to 10^{-5} M. This tube was shaken again. Next, 50 mL of ultrapure water was added to the tube containing the weighed $Fe(NO_3)_3 \cdot 9H_2O$ salt and shaken, creating a 10^{-3} M $Fe(NO_3)_3$ solution. Finally, 5 mL of this solution was added to the 45 mL $NaNO_3$ solution (for iron(III) only system) or the 45 mL

$NaNO_3$ and phosphate or arsenate solution, shaken, and immediately injected into the reaction cell. The final solutions contained 10 mM $NaNO_3$, 10^{-4} M $Fe(NO_3)_3$, and 10^{-5} M arsenate or phosphate. The reaction was considered to begin at the moment when ultrapure water was added to the weighed $Fe(NO_3)_3 \cdot 9H_2O$ salt. Taking this into account, only approximately two minutes elapsed between the start of the reaction and when the first GISAXS image was taken.

Preparing solutions and quartz powders for DLS and zeta potential measurements. For DLS and zeta potential measurements for homogeneously formed particles, solutions were prepared as outlined above. To measure the zeta potentials for the heterogeneously formed particles and for quartz in our different reaction systems, a quartz powder was used in place of the substrate. In a mortar and pestle, quartz was ground into fine particles. This powder was added to solutions created as outlined above, shaken, and set aside for 10 minutes to allow the larger quartz particles to settle from the suspension. Then the small, suspended quartz particles and upper region of solution were injected into the zeta potential cell. In addition, the zeta potential of the quartz powder itself was measured using the same procedure in 10 mM $NaNO_3$ and in the presence of the different concentrations of arsenate and phosphate. For these systems, the pH was adjusted to 3.6 ± 0.2 with nitric acid to match the pH of the reaction systems.

S2. Ex Situ Analyses of Iron(III) (Hydr)oxide Precipitate Nature

Measuring arsenate and phosphate content of precipitates. The solutions outlined in Table 1 were created following the above procedure, scaled up to a total volume of 500 mL in order to accumulate enough precipitation to achieve detectable iron and arsenic levels by ICP-MS. Solutions were reacted for 1 hour before beginning centrifugal filtration in small batches at 5000 RPM utilizing Millipore Amicon ultra-15 filter units. After the entire batch was filtered, the

precipitates on the filter were dissolved using a 2% nitric acid solution. The resulting solution was diluted, and arsenic and iron concentrations were measured using ICP-MS.

After filtration, each sample contained 250 μL of the 0.1 mM iron and 0.01 mM arsenic or phosphate solution. The concentrations of iron in the supernatant from the dissolved nanoparticles were ~1.6–3 mM for iron, ~0.2–0.5 mM for phosphorus, and ~0.1–0.3 mM for arsenic. These concentrations were obtained for 5 mL of the acidified solution. Therefore, the original solution contributed 0.000025 moles of iron and 0.0000025 moles of arsenic or phosphorus. These totals account for only 0.17–0.31% of the measured iron, 0.10–0.25% of the measured phosphorus, and 0.17–0.5% of the measured arsenic.

For heterogeneously formed precipitates, batch reactors were scaled up to contain 50 mL of the reaction solution. Quartz powder (103–381 μm) was added to maintain the same solution volume: surface area ratio as in the GISAXS batch reactor cell. The quartz powder was reacted for one hour in the iron only and arsenate- or phosphate-containing systems. The reactor contents were filtered and the quartz powder was rinsed using DI water. Iron (III) (hydr)oxide precipitates were dissolved using 2% nitric acid. The solution was passed through a 0.2 μm syringe filter and analyzed for iron, arsenic, and phosphorus concentrations using ICP-MS.

Determining phase of precipitates using Raman Spectroscopy and TEM. Raman spectroscopy was conducted on reacted GISAXS substrates using a Raman microscope (Renishaw, U.K.) with a 633 nm excitation wavelength. However, the only observable peaks were those of the quartz background due to the small quantity of precipitation on the substrate surface. In addition, we used high-resolution transmission electron microscopy (HRTEM) (JEOL JEM-2100F field emission, Tokyo, Japan) to observe homogeneously formed precipitates. For this testing, reaction solutions (Table 1) were prepared as outlined in the Supporting Information S1. After reaction for

1 hour, one drop of the solution was placed on a Formvar/carbon-coated Cu grid. Excess solution was dabbed off using a clean filter paper, and the grids were immediately analyzed using HRTEM to prevent sample aging. Precipitates on the grid were measured using electron diffraction, however no diffraction patterns were observed (Figure S4). Therefore, it is likely that these precipitates were amorphous during the early stages of nucleation and growth surveyed using *in situ* GISAXS measurements.

Determining ex situ precipitate phases using HRXRD. The solutions outlined in Table 1 were created following the above procedure, scaled up to a total volume of 1000 mL in order to accumulate enough precipitation for HRXRD measurements. Solutions were reacted for 1 hour before beginning centrifugal filtration in small batches at 5000 RPM utilizing Millipore Amicon ultra-15 centrifugal filter units. After the entire batch was filtered, the precipitates that accumulated on the filter were dried overnight in a desiccator. Samples were packed in Kapton capillary tubes and sent to 11-BM at APS for analysis using HRXRD. The total aging time of samples between when the reaction started and when the HRXRD measurements were conducted was 10−11days.

Beamline 11-BM at APS utilizes a Si(111) double crystal monochromator and a sagittally bent Si(111) Crystal and 1 meter Si/Pt mirror for horizontal and vertical focusing, respectively. The beam size is 1.5 mm wide and 0.5 mm tall. Diffraction is carried out using a Huber two-circle diffractometer, which contains 12 independent Si (111) crystal analyzers and $LaCl_3$ scintillation detectors. This set-up gives very high resolution ($\Delta Q/Q \approx 2\times10^{-4}$) in a very short time frame (~1 hour). The energy range for this instrument is 15–35 keV and the flux is $\sim5\times10^{11}$.

Water content of heterogeneous precipitates. For heterogeneously formed precipitates, *ex situ* samples were created on quartz substrate for the systems in Table 1. Substrates were immediately rinsed with deionized water and dried using high purity nitrogen. To determine the

sizes and morphology of newly-formed precipitates, these reacted substrates were imaged within 3 hours using AFM. To further examine the water content from the newly-formed precipitates, substrates were then dried in an oven at 100 °C for 24 hours and imaged again using AFM. Changes in particle size due to oven-drying were attributed to water loss from the newly-formed precipitates. For heterogeneously formed precipitates, we found that the particle size in the 10^{-4} M Fe(III) system and 10^{-4} M Fe(III)–10^{-5} M phosphate system remained similar before and after oven-drying, with sizes of 1–2 nm in both systems. For the 10^{-4} M Fe(III)–10^{-5} M arsenate system, particle size decreased after drying from 1–6 nm to 1–2 nm, which corresponds to volume reduction of up to 12.5% (Figure S3). The visible water loss from only the arsenate system is understandable given TGA analysis for the water content of the nanoparticles. According to the TGA data, the arsenate system had significantly more water content (21.6%) than the phosphate system and iron only system, which had 17.1% and 14.9% respectively.

Investigation of the effects of homogeneously formed particle settling. *Ex situ* experiments were conducted to show the effects of particle settling. Inverted (bottom up) *ex situ* batch systems were run for in the GISAXS fluid cell for 10 mM $NaNO_3$, 10^{-4} M $Fe(NO_3)_3$, and 10^{-5} M arsenate or phosphate. The morphology of precipitates on the quartz substrates in each system was analyzed using AFM (Figure S3). The inverted experiments demonstrate that the small precipitates observed on the mineral surface are from heterogeneous precipitation and not from the settling of small homogeneous precipitates, while the regular experiments demonstrate that there was not significant settling of heterogeneous precipitates.

S3. GISAXS Analyses

GISAXS experimental set-up and data analysis. Prior to running any samples, a *q* range calibration was done using a silver behenate standard. During GISAXS measurements, incident X-ray beams were passed through the GISAXS reaction cell, where they interacted with particles on the substrate surface (GISAXS). The scattered X-ray beams were collected by a 2-D detector, while those which passed through the solution hit the photodiode, which was constantly monitored for beam fluctuations or sample shifting during measurement. The incidence angle (α_i) between the incident X-ray beam and the substrate surface was chosen for these experiments to be 0.11°. This value was calculated, considering the substrate structure (quartz, α-SiO_2) and the beam energy (14 keV), to achieve a reflectivity of 98%. At this angle, the X-ray beam probed mainly nanoparticles on the substrate surface. For GISAXS measurements, X-ray scattering data was processed by cutting along the Yoneda wing. All data reduction was conducted using the GISAXSshop macro, available at APS beamline 12-ID-B. The data reduction procedure can be found in our previous publication.[1]

The scattering curves (I(q)) for each different time points (Figure 1) were fit using the following relationship:

$$I(q) = I_0 P_0(q, r_0, \sigma_0) S(q, I_{0s}, d, R_h, v_f). \quad S(1)$$

Within this relationship, P(q, R, σ) is the form factor. For our case, a polydisperse sphere model with the Schultz size distribution was used. This model was chosen because of the broad distribution in size and lack of form factor oscillations in the scattering curves.

The structure factor appears in this relationship as $S(q, I_{0s}, d, R_h, v_f)$. This factor can be broken down into two parts as follows for the large aggregate system composed of small primary particles:

$$S(q, I_{0s}, d, R_h, v_f) = I_{0s}q^d + S(q, R_h, v_f). \quad S(2)$$

Within this equation, $I_{0s}q^d$ models the Porod scattering from the aggregates. I_{0s} is a scaling constant and d is the Porod power-law exponent. The term $S(q, R_h, v_f)$ represents the internal structure of the aggregates made of the primary particles, or the structure factor for the primary particles. The hard-sphere Percus-Yevick model was used for the $S(q, R_h, v_f)$, wherein R_h is the hard-sphere interaction radius and v_f is the volume fraction.

Calculation of precipitate electron densities. During GISAXS analyses for the relative total particle volume comparison, we also considered the effects of arsenate and phosphate incorporation on the electron density. Increases in the electron density due to arsenic incorporation would increase the electron density of the particles, leading to higher GISAXS scattering intensities. However, this increase cannot be attributed to differences in precipitate quantities between the systems. Using the measured arsenic incorporation quantities for the homogeneous precipitates, the electron densities were calculated to be 1.12 e/Å^3 for the Fe(III) only system, 1.20 e/Å^3 for the system containing 10^{-5}M arsenate, and 1.34 e/Å^3 for the system containing 10^{-5} M phosphate. The contrast between the precipitates and water was calculated to be

$$Contrast = (\rho_{precipitate} - \rho_{water})^2. \quad S(3)$$

The contrasts for the 10^{-4} M Fe(III), 10^{-4} M Fe(III)–10^{-5} M arsenate, and 10^{-4} M Fe(III)–10^{-5} M phosphate systems were calculated to be 0.6260, 0.7531, and 1.022 respectively. The GISAXS

intensity is proportional to both the contrast and the total volume of particles according to the following relationship:

$$Intensity = constrast \times no.of\ particles \times individual\ particle\ volume. \quad \text{S(4)}$$

Therefore, the ratios of the intensities and contrast were compared for the 10^{-4} M Fe(III) (standard system) and 10^{-4} M Fe(III)–10^{-5} M arsenate or 10^{-4} M Fe(III)–10^{-5} M phosphate systems. While the contrast for the arsenate system was 1.2 times the intensity for the iron standard system, the scattering intensity for arsenate was 18 times higher. For the phosphate system, the contrast was 1.6 times higher and the scattering intensity was 5 times that of the iron standard system.

Fitting of GISAXS Data. When analyzing GISAXS data from polydisperse particles, the shape of particles is assumed to be spherical unless their shape is well defined. Due to the nature of this system, the size distribution and shape cannot be determined independently. For polydisperse spherical particles, the form factor is written as

$$P(q) = \Delta\rho^2 \int_0^\infty n(r)\left|F_{sphere}(q,r)\right|^2 dr, \quad \text{S(5)}$$

where $n(r)$ is the size distribution function and $F_{sphere}(q,r)$ is the scattering amplitude of a sphere with radius r. For $n(r)$, typically a function with a minimal number of parameters is preferred. One common size distribution function is the Schultz distribution, which is

$$n(r;\, r_0, z) = \left(\frac{z+1}{r_0}\right)^{z+1} r^z e^{-\frac{(z+1)}{r_0}r} / \Gamma(z+1). \quad \text{S(6)}$$

The Schultz function is defined by two parameters, r_0 and z, where r_0 is the mean radius and Z is related to the variance of the radii. The root mean square deviation from the mean is given by

$$\sigma_R = r_0/(z+1)^{1/2}. \quad \text{S(7)}$$

When the Schultz distribution function is used as a size distribution, GISAXS intensity can then be calculated analytically as follows:

$$P(q) = 8\pi\Delta\rho^2 r_0^6 (z+1)^{-6} \alpha^{z+7} G_1(q), \quad \text{S(8)}$$

where

$$G_1(q) = \alpha^{-(z+1)} - (4+\alpha^2)^{-\frac{z+1}{2}} \cos\left((z+1)\tan^{-1}\frac{2}{\alpha}\right)$$

$$+(z+1)(z+2)\left(\alpha^{-(z+3)} + (4+\alpha^2)^{-\frac{z+3}{2}} \cos\left((z+3)\tan^{-1}\frac{2}{\alpha}\right)\right)$$

$$-2(z+1)(4+\alpha^2)^{-\frac{z+2}{2}} \sin\left((z+2)\tan^{-1}\frac{2}{\alpha}\right) \quad \text{S(9), and}$$

$$\alpha = (z+1)/(qr_0). \quad \text{S(10)}$$

The calculated GISAXS intensity can then be compared to the measured GISAXS intensity, and a number of variables are tuned using a MATLAB fitting program to achieve the best fit. Once the best fit is achieved, Rg is calculated using

$$\mathrm{R_g} = \frac{3}{5} r_0 \frac{\sqrt{(z+8)(z+7)}}{z+1}. \quad \text{S(11)}$$

Polydispersity of heterogeneous precipitates. Polydispersity was estimated by dividing σ by r_0. Both of these factors are outputs of the fitting described above. The polydispersity changes for the three systems over the first hour of reaction can be found in Figure S7. These results indicate that the arsenate system had the smallest distribution of particles, while the distributions for the iron only and phosphate systems were similar. For the arsenate only system, most of the particles were close to the average size value of 6.1 nm. For the phosphate and iron only systems, particle sizes were more widely scattered around their average values of 4.0 nm and 2.5, respectively.

Reference

1. Jun, Y.-S.; Lee, B.; Waychunas, G. A., In Situ Observations of Nanoparticle Early Development Kinetics at Mineral - Water Interfaces. Environmental Science & Technology 44, (21), 8182-8189.

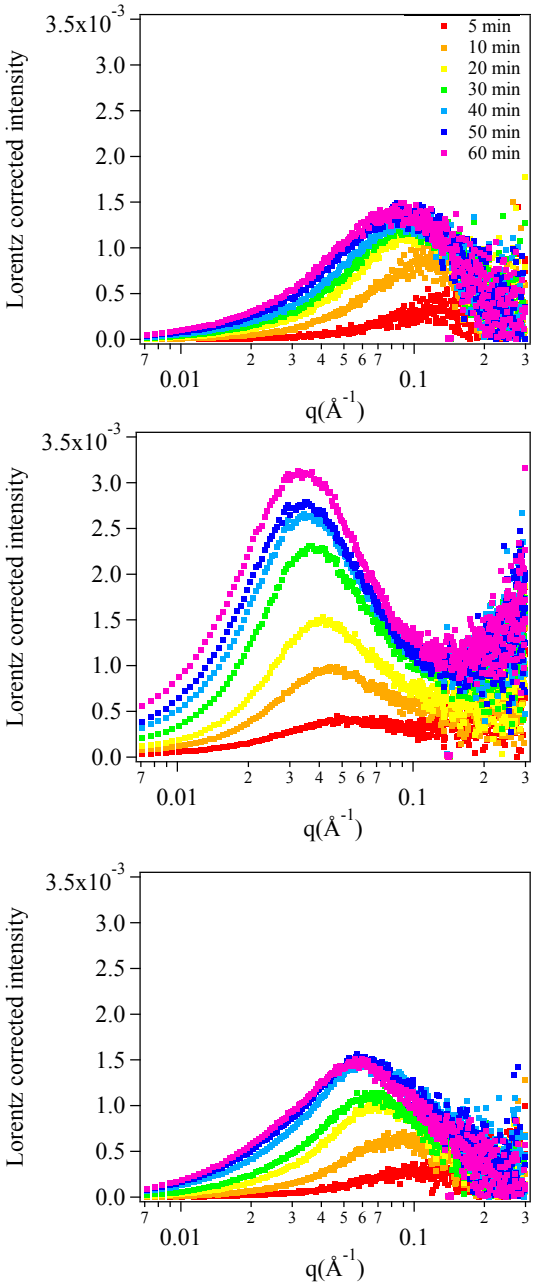

Figure S1. Lorentz corrected scattering intensities for heterogeneously formed particles on quartz in the systems containing 10 mM sodium nitrate with (A) 10^{-4} M Fe(III), (B) 10^{-4} M Fe(III) and 10^{-5} M arsenate, and (C) 10^{-4} M Fe(III) and 10^{-5} M phosphate.

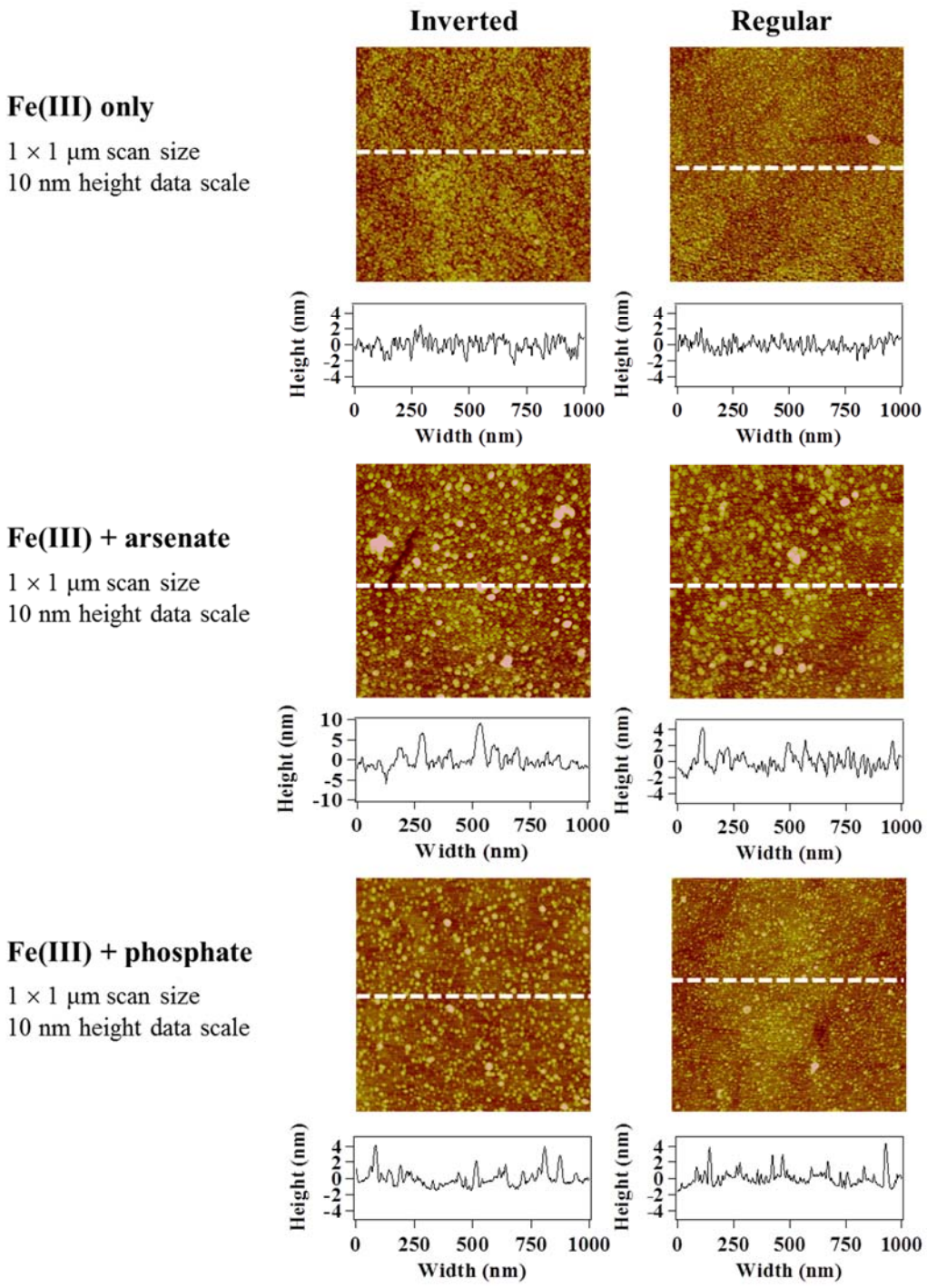

Figure S2. Comparison of surface morphologies in regular and inverted set-up experiments. AFM has a vertical resolution on the sub-angstrom scale, while lateral resolution for tapping mode is ~40 nm, significantly larger than the precipitate size. Therefore, the vertical dimensions measured by sectioning of height mode images were used to define *ex situ* particle sizes for the various experimental systems.

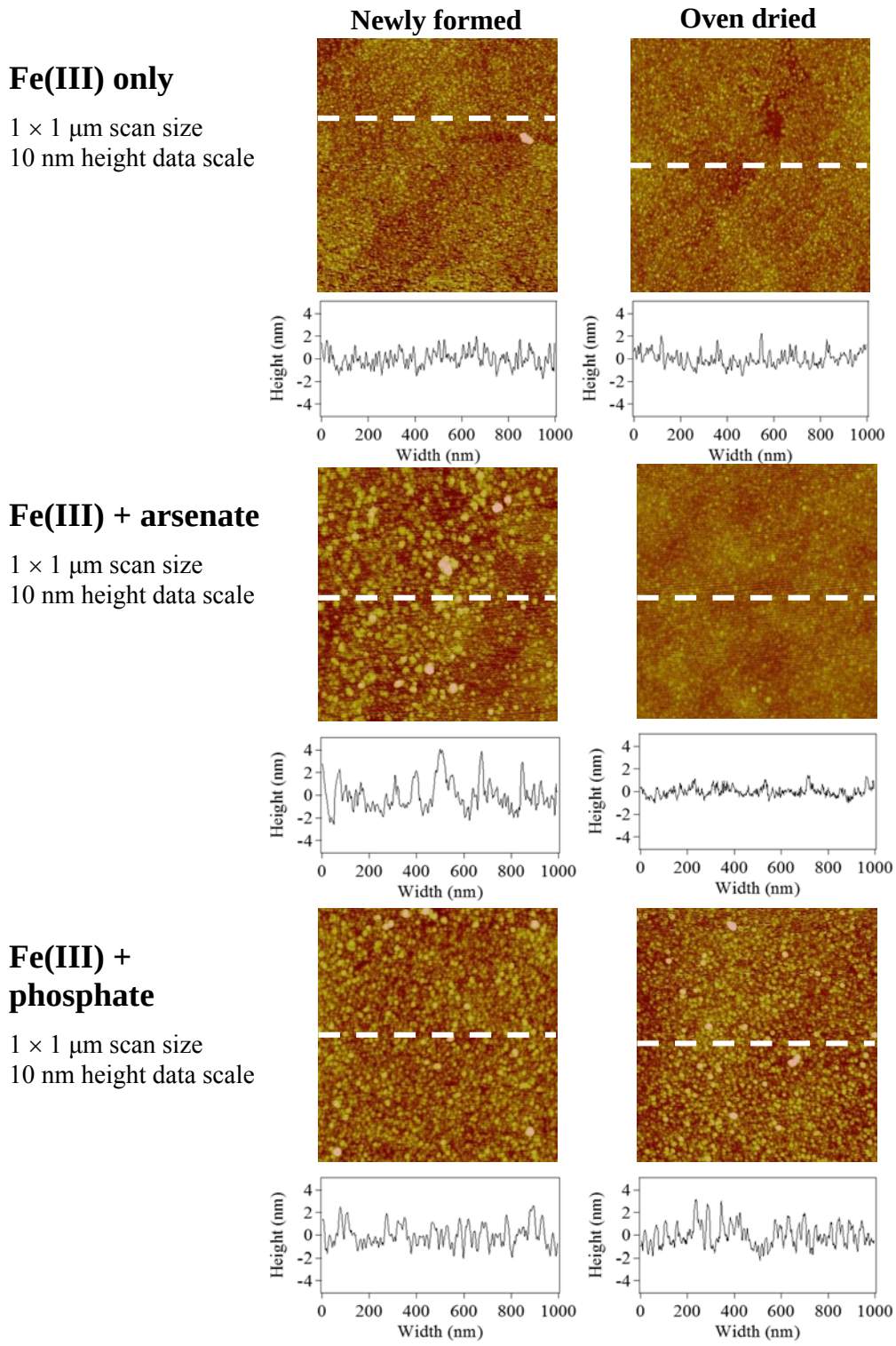

Figure S3. AFM Images and height sections showing the difference in particle size for newly formed heterogeneously formed precipitates and precipitates which were dried in an oven at 100 °C for 24 hours. There was observable particle shrinking only in the system which contained arsenate.

Figure S4. Electron diffraction pattern for homogeneous precipitates in the system containing Fe(III) and arsenate. No diffraction pattern was observed for any system, indicating that all precipitates were amorphous in the early stages of nucleation and growth.

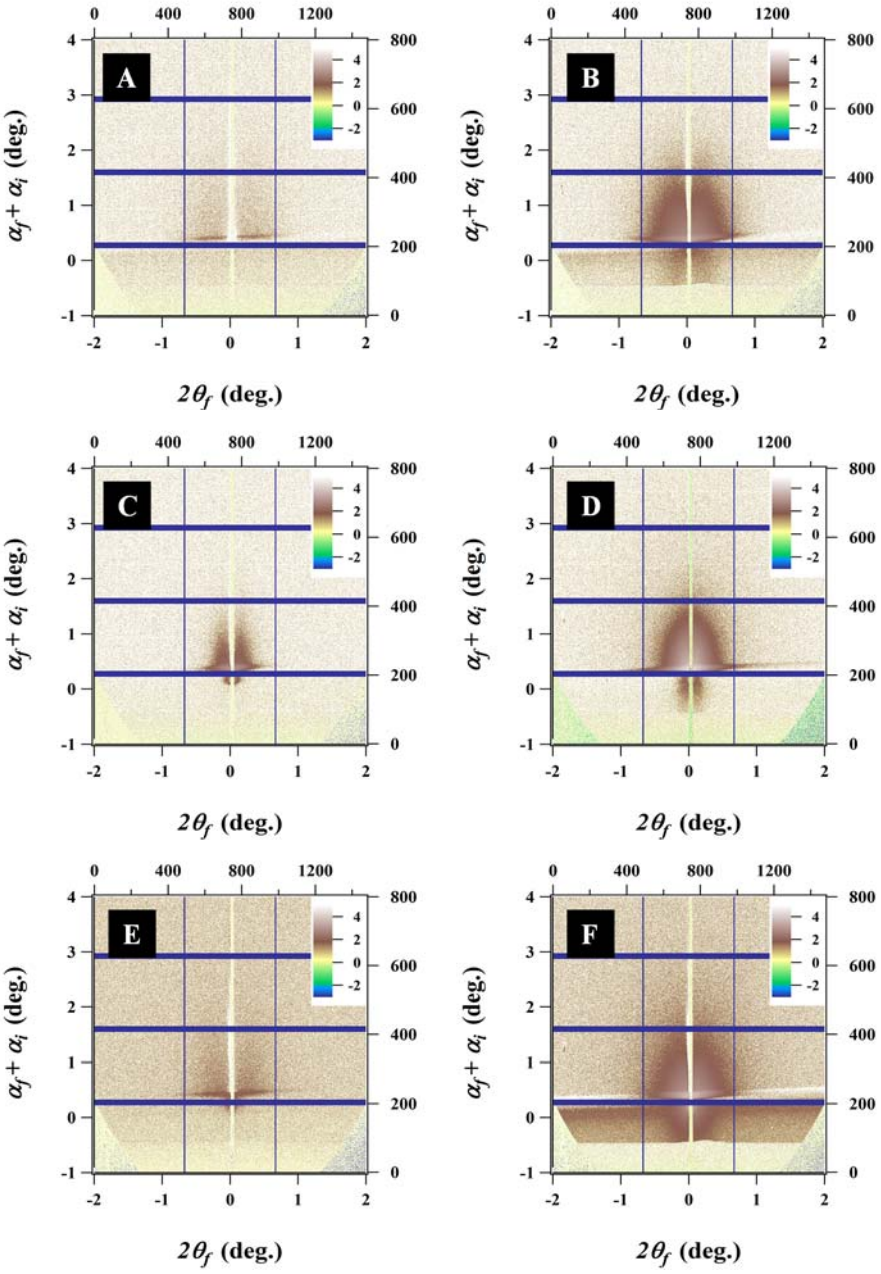

Figure S5. 2D scatting images for the Fe(III) only system after (A) 5 minutes and (B) 60 minutes, the iron + arsenate system after (C) 5 minutes and (D) 60 minutes and the iron and phosphate system after (E) 5 minutes and (F) 60 minutes.

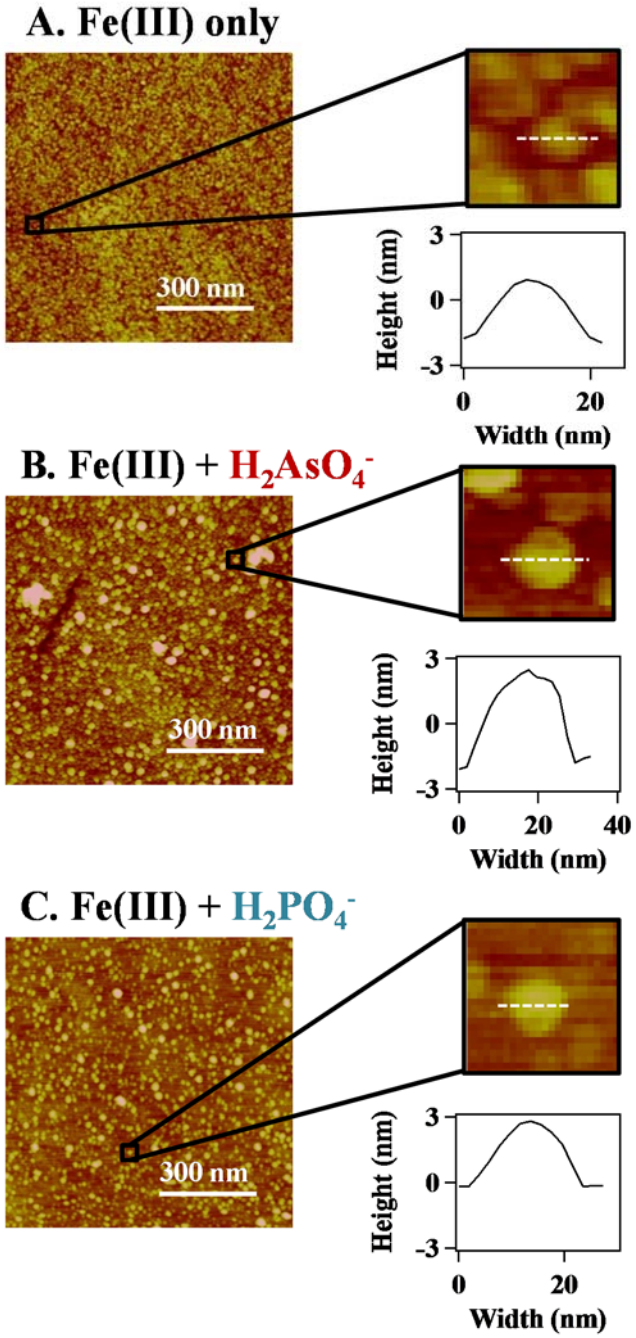

Figure S6. AFM line cuts of single particles on the quartz background for (A) the Fe(III) only system, (B) Fe(III) + arsenate system, and (C) Fe(III) + phosphate system.

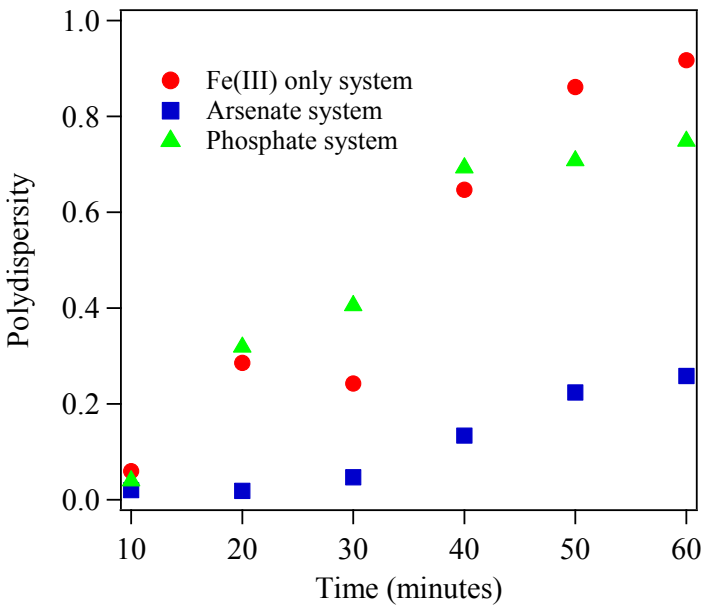

Figure S7. Polydispersity changes for the Fe(III) only, arsenate, and phosphate systems over the one hour reaction period.